ISTANBUL TECHNICAL UNIVERSITY ★ GRADUATE SCHOOL OF SCIENCE

ENGINEERING AND TECHNOLOGY

COUNTER ALIGNING INCLINATION ANGLE OF CRAB PULSAR WITH DECREASING MOMENT OF INERTIA

M.Sc. THESIS

İbrahim Ceyhun ANDAÇ

Department of Physics Engineering

Physics Engineering Programme

MAY 2015

ISTANBUL TECHNICAL UNIVERSITY ★ GRADUATE SCHOOL OF SCIENCE
ENGINEERING AND TECHNOLOGY

COUNTER ALIGNING INCLINATION ANGLE OF CRAB PULSAR WITH DECREASING MOMENT OF INERTIA

M.Sc. THESIS

İbrahim Ceyhun ANDAÇ
(509121107)

Department of Physics Engineering

Physics Engineering Programme

Thesis Advisor: Prof. Dr. Kazım Yavuz EKŞİ

MAY 2015

İSTANBUL TEKNİK ÜNİVERSİTESİ ★ FEN BİLİMLERİ ENSTİTÜSÜ

YENGEÇ ATARCASININ AZALAN EYLEMSİZLİK MOMENTİYLE AÇILAN EĞİKLİK AÇISI

YÜKSEK LİSANS TEZİ

İbrahim Ceyhun ANDAÇ
(509121107)

Fizik Mühendisliği Anabilim Dalı

Fizik Mühendisliği Programı

Tez Danışmanı: Prof. Dr. Kazım Yavuz EKŞİ

MAYIS 2015

İbrahim Ceyhun ANDAÇ, a M.Sc. student of ITU Graduate School of Science Engineering and Technology with student ID 509121107 has successfully defended the thesis entitled **"COUNTER ALIGNING INCLINATION ANGLE OF CRAB PULSAR WITH DECREASING MOMENT OF INERTIA"**, which he prepared after fulfilling the requirements specified in the associated legislations, before the jury whose signatures are below.

Thesis Advisor :	**Prof. Dr. Kazım Yavuz EKŞİ** Istanbul Technical University	....
Jury Members :	**Assoc. Prof . Dr. Abdurrahman Savaş ARAPOĞLU** Istanbul Technical University	....
	Assoc. Prof . Dr. Tolga GÜVER Istanbul University	....

Date of Submission : **04 May 2015**
Date of Defense : **26 May 2015**

FOREWORD

Firstly, I would like to thank my advisor, K. Yavuz EKŞİ, who has been supporting me for my undergraduate times up to now. It is a pleasure to work with him, with his inclusive view, assistance and wisdom. I would like to thank Erbil Gügercinoğlu and Prof. Dr. Ali Alpar who have been supporting and helping to develop our idea, which forms the subject of this thesis, from the beginning . I would also like to thank my family for their limitless credits about my interest in science whether they are next to me as it was twenty years ago, or they are far away. I would like to thank 'İTÜ Fizik Haftası Crew'. They have teach to me, learned with me, thought with me on physics, nature and its language mathematics. It feels very good to know that whenever I want to deal with physics, I don't have to do it alone. I again would like to thank to Prof. Dr. K. Yavuz EKŞİ for founding our home, High Energy Astrophysics Laboratory (HEAP), and my 'home mates', for their friendship and helpful advises. I am thankful to Küpçük's experience about professional thesis writing and his own existence and Buğra Tüzemen's simultaneous friendship. And lastly, I would like to thank my beloved, Yaşam Çağlar, for her patience and love.

May 2015 İbrahim Ceyhun ANDAÇ

TABLE OF CONTENTS

Page

ABBREVIATIONS

NS	**:** Neutron Star
RPP	**:** Rotational Powered Pulsar
MDR	**:** Magnetic Dipole Radiation
MHD	**:** Magnetohydrodynamics
ATNF	**:** Australia Telescope National Facility
AXP	**:** Anomalous X-Ray Pulsar
SGR	**:** Soft Gamma-Ray Repeater
RRAT	**:** Rotational Radio Transient
INS	**:** Isolated Neutron Star
SN	**:** Supernova
SNR	**:** Supernova Remnant

LIST OF FIGURES

Page

LIST OF SYMBOLS

c	: speed of light
I	: moment of inertia
μ	: dipole magnetic moment
Ω	: angular velocity
α	: inclination angle
τ_c	: characteristic age
τ_I	: time scale of moment of inertia change
n	: braking index
m	: second braking index
n_{I}	: rate of change of I similar with braking index
m_{I}	: rate of change of I similar with second braking index

COUNTER ALIGNING INCLINATION ANGLE OF CRAB PULSAR WITH DECREASING MOMENT OF INERTIA

SUMMARY

A star with a mass between $8-22\,M_{\odot}$ becomes a neutron star when it has used up all of its nuclear energy sources. This transition occurs with a gigantic supernova explosion. Today there are many types of neutron stars classified according to their energy source. The first discovered neutron stars are the rotationally powered pulsars. These are highly magnetized rapidly rotating objects which are slowly spinning down, and the rate of rotational kinetic energy lost forms their luminosity. These objects, presumably the younger ones, radiate in all bands of the electromagnetic spectrum yet they are generally detected in the radio wavelength. The first models envisaged the pulsars as a magnetic dipole rotating in vacuum converting the kinetic energy to magnetic dipole radiation (MDR). It was soon understood that the rotating dipole generates electric fields large enough to rip off charged particles from the surface of the neutron star which then form a co-rotating plasma. It is harder to solve the magnetospheric structure in the presence of this plasma, but recent numerical simulations provide insight into this problem. Even in that case, the basic dependence of the spin-down torque on the pulsars in the presence of the plasma is similar to the MDR model. Interestingly both models predict that the inclination angle between the magnetic moment and the spin axis would be aligned in time.

The Crab pulsar is the best known and studied rotationally powered pulsar among the more than 2000 pulsars discovered to date. It is about 960 years old according to the ancient Chinese records, which call the supernova explosion as a ‘guest star’. Lyne et al. discovered in 2013 that the inclination angle of this object is not decreasing, as expected from the MDR or the plasma model, but increasing at a rate of 0.62 degrees per century. We argue that this observation can be explained if the moment of inertia of this object decreases in time. In standard estimations of pulsar properties the moment of inertia and magnetic dipole moment are assumed to be constant. In this thesis, I investigate the implications of a decrease in the moment of inertia on the spin evolution of this object.

The Crab pulsar, just like many other young pulsars, occasionally show sudden spin-up events called “glitches”. The glitch events of the Crab pulsar are explained by the starquake model. According to this model the solid crust of the Crab pulsar, which is formed when the object cooled down while rotating much more rapidly, can not follow the equilibrium shape corresponding to the rotation rate which slowed down. The stress increases as the pulsar slows down further and finally the crust of the neutron star fractures. Recently, we had shown that the rate of decrease of the moment of inertia as a result of these crustal fractures is sufficient to explain the rate of increase of the inclination angle.

YENGEÇ ATARCASININ AZALAN EYLEMSİZLİK MOMENTİYLE AÇILAN EĞİKLİK AÇISI

ÖZET

Yıldızlar da doğar, büyür ve ölürler. Güneş ve diğer yıldızlar gibi nükleer tepkimeler sayesinde enerji üreten ve ışık saçan yıldızlar, "büyüme" dönemlerini geçirmektedirler. İşte bu dönemden sonra yıldızlar kütlelerinin getirdiği biçimde, kimileri çok hızlı, kimileriyse daha yavaş olmak üzere ölmeye başlarlar. $8-22\ M_{\odot}$ kütleli bir yıldız tüm nükleer enerji kaynaklarını tükettiğinde bir nötron yıldızına dönüşür. Bu geçiş devasa bir süpernova patlaması ile gerçekleşmektedir; öyle ki, güneş haricindeki neredeyse tüm göksel nesneler yalnızca gece karanlığında görülebilirken, bir süpernova patlaması parlaklığının büyüklüğü sayesinde güneşli havada bile gözlenebilen bir astrofiziksel olaydır. Nötron yıldızlarının oluşma mekanizmaları benzerdir fakat temel enerji kaynakları farklılık gösterebilir. Günümüzde, enerji kaynaklarının çeşidine göre sınıflanan birçok nötron yıldızı vardır. İlk keşfedilen nötron yıldızları ışıma gücünü dönme kinetik enerjisinden alan atarcalardır. Bu atarcaların da ilki Anthony Hewish ve onun doktora öğrencisi Jocelyn Bell tarafından 1967 yılında keşfedilmiş, bu keşif Anthony Hewish'e 1974 yılı Nobel Fizik Ödülü'nü kazandırmıştır. Atarcalar, manyetik özelliği oldukça kuvvetli (10^8 Gauss ile 10^{15} Gauss arasında değişen), gittikçe yavaşlamakla beraber hızlıca dönen nesneler olup dönme kinetik enerjilerindeki kayıp oranı, onlara ışıma güçlerini kazandırmaktadır. Bu nesneler, özellikle genç olanları, genelde radyo dalgaboyunda saptanmaktadırlar fakat aslında elektromanyetik tayfın tüm dalga boylarında ışıma yapmaktadırlar. Bu olguyu açıklayan ilk modeller atarcaları, kinetik enerjilerini manyetik dipol ışımasına (MDR) dönüştüren, boşlukta dönen manyetik dipoller olarak ortaya koymaktadırlar. Kısa süre sonra anlaşılmıştır ki dönen bir manyetik dipol, nötron yıldızının yüzeyinden, koptuktan sonra yıldızla birlikte dönen bir plazma meydana getirecek yüklü parçacıkları söküp alabilecek denli büyük elektrik alanlar indüklemektedir. Nitekim dönen bir nötron yıldızının boşlukta değil, plazma içinde bulunması gerektiği de 1969 yılında Goldreich ve Julian tarafından gösterilmiş, atarcaların içinde bulunduğu bu plazma manyetosferin yoğunluğuna da ρ_{GJ} (Goldreich ve Julian yoğunluğu) denilmiştir. Bu plazmanın varlığında manyetosferik yapıyı çözmek daha zor hale gelmektedir fakat son yapılan sayısal benzeşimler bu problemin iç yüzünün de anlaşılmasını sağlamıştır. Plazmanın varolduğu durumda bile, yavaşlamanın doğurduğu dönme momentinin MDR modelindekine benzerlik gösterdiği görülmektedir. Minimum enerji prensibine bağlı olarak her iki model de manyetik moment ve dönme ekseni arasındaki eğiklik açısının zamanla kapanacağını öngörmektedirler.

Yengeç (Crab) atarcası, bugüne kadar keşfedilmiş, sayıları 2000'in üzerindeki dönme kinetik enerjisiyle güçlenen atarcalar içinde en iyi bilineni ve en çok çalışılanıdır. Yengeç atarcası üzerine internet arşivlerinde bugüne değin yayınlanmış çalışmalar beş haneli sayılara ulaşmak üzeredir. Bu da, Yengeç atarcasının doğumundan bugüne dek

kaydının tutulmasından ileri gelmektedir. Bu atarca, dünya takvimiyle M.S. 1054 yılında, oluştuğu süpernova patlamasını bir ‘misafir yıldız’ olarak kaydetmiş olan antik Çin kayıtlarına göre yaklaşık 960 yaşındadır. Bu patlama ve sonrasında çok daha hızlı dönüyor olmakla beraber, Yengeç atarcası günümüzde 33 ms periyotla dönmekte ve saniyede 4.21×10^{-13} saniye periyot türevi ile yavaşlamaktadır.

Nötron yıldızlarının yukarıda bahsedilen büyük manyetik alanları onları tanımlayan çok önemli özelliklerinden biridir. Elektrik alanları, kütlelerinin büyük kısmını nötronlar ya da elektron-proton çiftleri oluşturduğundan daha çok manyetik alanın indüklediği elektrik alanlar olarak öne çıkarlar. Nötron yıldızlarının manyetik alanları, nötron yıldızlarının yarıçaplarının küçük olmalarından etkilendikleri gibi, aynı zamanda farklı mekanizmalarla oluşup desteklenirler. Bu sebeple nötron yıldızlarının izole ya da tek olmaları, yaşları ve dönüş hızları manyetik alanlarının varoluşunu büyük oranda etkilemektedir. Söz gelimi magnetar adı verilen çok büyük manyetik alanlı nötron yıldızları, isimlerinden de anlaşılabileceği gibi manyetik alanlarının büyüklükleri ile öne çıkmışlardır. Görece daha yavaş periyotlarla dönen bu nötron yıldızı tiplerinin manyetik alanları dipol yapıda değildir. Dipol yapısı baskınlık göstermeyen başka tip nötron yıldızları da vardır fakat nötron yıldızları, özellikle atarcalar genelde dipol manyetik alan etkisi yüksek olan cisimlerdir. Bir manyetik dipol, bilindiği üzere, yönlü bir manyetik momente sahiptir. Atarcaların manyetosferlerinde plazmanın varlığı gösterilmiş olsa da, daha rahat anlaşılır olmasından ötürü yaygın olarak kullanılan MDR modeli, nötron yıldızlarının dönme kinetik enerjilerini manyetik dipol ışımasından aldıklarını öne sürer. Bu modele göre manyetik dipol dönme momentinin iki bileşeni bulunmaktadır. Bunların biri açısal hızın değişimiyle gelen terimdir:

$$\frac{d}{dt}(I\Omega) = -\frac{2\mu^2\Omega^3}{3c^3}\sin^2\alpha.$$

Birçok başka atarca gibi Yengeç atarcasının da manyetik dipol ekseni ile dönüş ekseni birbirinden farklıdır. Bu iki eksen arasındaki açıya ”eğiklik açısı“ denir. Bu eğiklik açısının değişimiyle de ikinci dönme momenti terimi bulunur:

$$\frac{d}{dt}(I\alpha) = -\frac{2\mu^2\Omega^2}{3c^3}\sin\alpha\cos\alpha.$$

Lyne ve ark.’nın 2013 yılında yaptıkları, 22 yıllık bir gözlemi analiz edip ulaştıkları sonuçlar göstermektedir ki, Yengeç atarcasının eğiklik açısı MDR ya da plazma modellerinde beklendiği üzere azalmamakta, tam aksine yüz yılda 0.62 derece oranında artmaktadır. Bu iki bileşende de eylemsizlik momentinin zaman içinde değişmediği gözönüne alınır ve hem eğiklik açısının hem de açısal hızın yavaş yavaş azaldığı kanısı yaygındır. Biz bu gözlemin, bu nesnenin eylemsizlik momentinin zaman içinde azalmasıyla açıklanabileceğini iddia ediyoruz çünkü azalan eylemsizlik momenti her iki bileşen için de pozitif terimler getirir. Burada kafa karıştırıcı olan, açısal hızdaki artışın da, eğiklik açısını arttıran eylemsizlik momentiyle doğru şekilde artıp artmayacağıdır. Bu tezde, azalan dönme momentinin Yengeç atarcasının dönüşünün zaman içindeki evrimine etkilerini inceledik. Tezde bahsedilen evrim, nötron yıldızlarının gözlenebilen parametreleri olan frenleme indisi, ikincil frenleme indisi, manyetik moment gibi değişkenlerin eğiklik açısına, açısal hıza ve birbirlerine göre durumları üzerinden anlaşılmaya çalışılmıştır.

Atarcalar için birçok keşif, onların atma profillerinin uzun süren gözlemlerinin analizleri sonucunda yapılabilmektedir. Yengeç atarcası da, diğer birçok genç atarca gibi zaman zaman dönüşünde “glitch” (arıza) denilen ani hız artışları gösterir. Atma profilinde gözlenen bu arızalar yıldız depremi modeliyle açıklanmaktadır. Bu modele göre, Yengeç atarcasının çok daha hızlı döndüğü ve bu sebeple daha hızlı da soğuduğu ilk zamanlarında sertleşmiş olan kabuğu, artık yavaşlamış dönüş hızı yüzünden şeklini muhafaza edemez. Atarca daha da yavaşladıkça gerginlik artar. Sonunda kabuk kırılır ve büyük bir deprem meydana gelir. İlk kırılma çok zor gerçekleşir fakat daha sonraki kırılmalar ve bu kırılmaların doğurduğu depremler daha kolayca ve sıkça oluşurlar. Kısa süre önce göstermiş bulunmaktayız ki, kabuk kırılmalarının sonucu olan eylemsizlik momentindeki azalma, Yengeç atarcasının eğiklik açısında gözlenmiş olan artışı açıklamaya yeterli büyüklüktedir.

1. INTRODUCTION

When a star with a mass in the range $\sim 8-20\,M_\odot$ consumes its nuclear energy creating thermal pressure, the balance between gravitation and thermal pressure is broken down. Neutron stars (NS) are collapsed remnants of these stars. The collapse of the core is accompanied by a spectacular supernova (SN) explosion, as first argued by Baade and Zwicky in 1934 [1]. If the mass of the star before death is bigger than $\sim 20\,M_\odot$ a black hole (BH) is expected to form. Stars with initial mass less than $8\,M_\odot$ become white dwarfs (WDs).

A NS has a radius about 10 km, and a mass up to $2-3\,M_\odot$. Accordingly, gravitational acceleration on the surface is about $g \simeq 1.9\times 10^{14}\,\mathrm{cm\ s}^{-2}(M/1.4M_\odot)(R/10\ \mathrm{km})^{-2}$ and the average density is $\bar{\rho} \simeq 6.7\times 10^{15}\ \mathrm{g/cm}^3(M/1.4M_\odot)(R/10\ \mathrm{km})^{-3}$. A typical young neutron star has a magnetic field $B \sim 10^{12}$ Gauss. The hydrostatic equilibrium of a neutron star is provided by the neutron degeneracy pressure of the interacting neutrons.

Neutron stars have many astrophysical manifestations with different mechanisms for their radiative output. The first discovered [2] type of neutron star, radio pulsars, are rotationally powered [3] i.e. they derive their radiative output from their rotational kinetic energy. Pulsars were discovered in 1967 by Jocelyn Bell, then a graduate student, and her advisor Anthony Hewish who was awarded the Nobel Prize in 1974 [2]. Up to now, more than 2000 rotationally powered pulsars are discovered. In 1971 X-ray pulsars were discovered in binary systems. These are gravitationally powered neutron stars accreting mass from their companion. Apart from these canonical manifestations there are more recently identified neutron star classes. These young neutron star families include anomalous X-ray pulsars (AXP), soft gamma-ray repeaters (SGR), rotating radio transients (RRAT), X-ray dim isolated NSs (XDINs) and central compact objects (CCO). Of these AXPs and SGRs are commonly accepted to be magnetars i.e. magnetically powered NS. RRATs are most likely rotationally powered. XDINs and CCOs most likely emit their thermal energy.

Of the more than 2000 pulsars discovered to date the Crab pulsar rotating at the center of the Crab nebula is the most well known and studied object. The SN explosion of the Crab nebula was detected by ancient Chinese astronomers in 1054. By this record, we know that the Crab pulsar is about 961 years old presently.

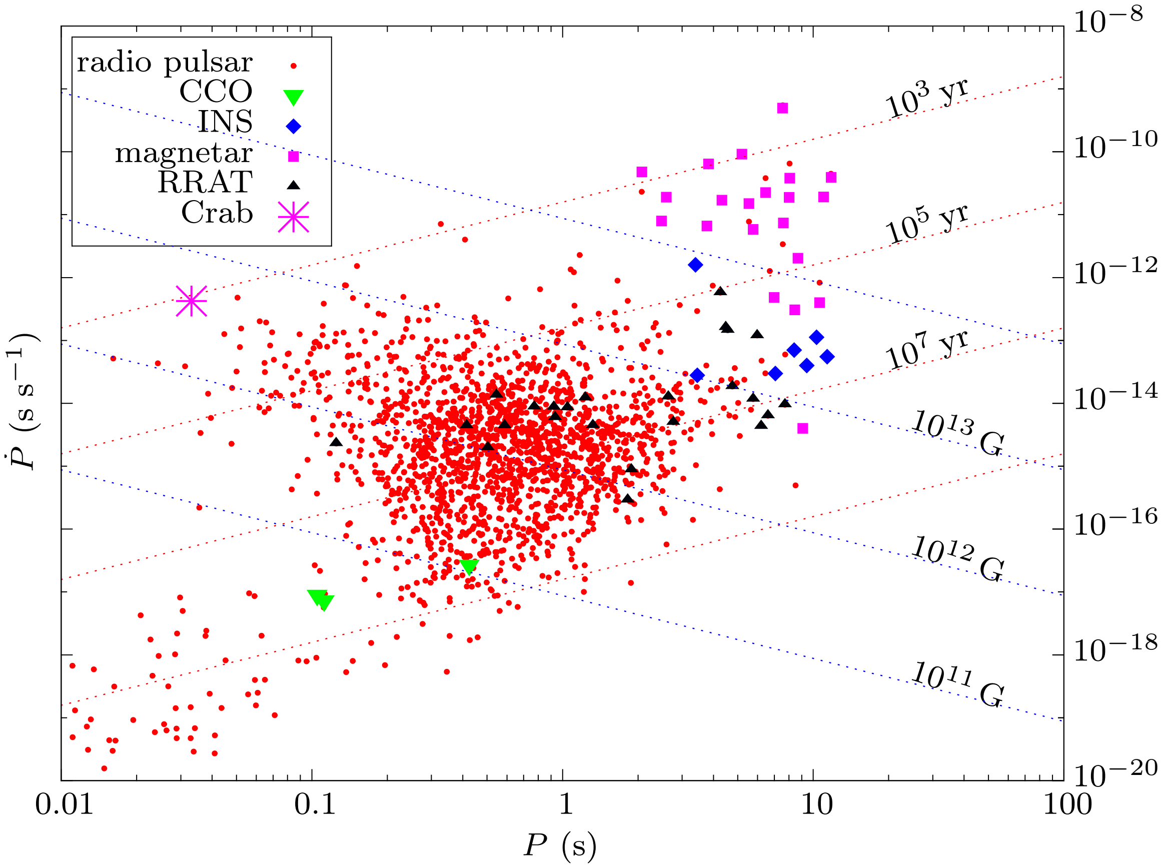

Figure 1.1: $P-\dot{P}$
P-Pdot diagram for isolated pulsars. This figure includes almost all observed radio pulsars, CCOs, INSs, RRATs, magnetars. Dashed slope lines are neutron star age and magnetic field lines.

The inclination angle between the spin axis and the magnetic moment axis of the Crab pulsar is constrained to be $45^\circ - 70^\circ$ [4–7]. In 2013, with 22 years of observation, Lyne et al. [8] has shown that the Crab Pulsar's inclination angle is increasing at a rate of $0.62^\circ \pm 0.03^\circ$ per century. This means that the Crab pulsar's magnetic moment axis is counter-aligning. This observation is contrary to the view that the inclination angle should decrease on energetic grounds. There are several ideas which claim that the inclination angle should decline; for instance pulsars are also spun-down by torques caused by open field lines of the magnetosphere and the return current on the NS surface could cause counter-alignment of the inclination angle [9].

The observed increase in the inclination angle might be a consequence of the change of the moment of inertia. Such a change in the moment of inertia of a NS may probably be caused by star-quakes. Star-quakes are related with pulsar glitches [10] which are sudden spin-ups. As these glitches occur, the crust of NS becomes more spherical and the moment of inertia (I) decreases.

In this thesis, the MDR model would be introduced as basis. Spin [11, 12] and inclination angle [13] evolution of pulsars in plasma medium will be considered. Finally, the plasma-filled magnetosphere model will be modified by allowing moment of inertia to change. The implications of this model for the Crab pulsar and rotationally powered pulsars in general will be investigated.

2. MAGNETIC DIPOLE RADIATION MODEL

In this chapter, I introduce the basics of the magnetic dipole radiation model (MDR) for RPPs.

2.1 Basic model with vacuum medium

Soon after their discovery pulsars were identified as rapidly rotating magnetized neutron stars [3]. The possibility that the Crab nebula is energized by such an object was already discussed before the discovery [14, 15]. It was suggested that MDR is the mechanism converting rotational energy to radiation. Explicit solutions for magnetic and electric fields around a magnetized conducting sphere, in the context of ordinary stars was already given by Deutsch (1955) [16] long before the discovery of RPPs.

A neutron star with moment of inertia I has a rotational kinetic energy

$$E_{rot} = \frac{1}{2} I \Omega^2 \tag{2.1}$$

where Ω is the angular velocity. As the object slows down, the rate of change of the rotational kinetic energy is

$$\frac{dE_{rot}}{dt} = I\Omega\dot{\Omega} \tag{2.2}$$

where we assumed I is constant. The rate at which the energy is radiated by MDR is

$$\frac{dE_{rot}}{dt} = -\frac{B^2 R^6}{6c^3}\Omega^4 \sin^2\alpha \tag{2.3}$$

[3, 15] where α is the inclination angle between rotation and magnetic axis and c is the speed of light. At the poles, the magnetic field of a conducting sphere is

$$B_p = \frac{2\|\vec{\mu}\|}{R^3} \tag{2.4}$$

[17] where μ is the magnetic moment and B_p is the polar component of the magnetic field of neutron star. If we plug Equation **2.4** into Equation **2.3** and equate it with Equation **2.2** we obtain

$$\frac{d}{dt}(I\Omega) = -\frac{2\mu^2\Omega^3}{3c^3}\sin^2\alpha, \tag{2.5}$$

Table 2.1: Pulsar Data

Period, characteristic age and braking index values of well-observed pulsars

Pulsar Name	Period(s)	τ_c(kyr)	n	Reference
B0531+21 (Crab)	0.033	1.2568	2.51±0.01	[8, 24]
B0833-45 (Vela)	0.089	11.322	1.4±0.2	[25, 26]
J1833-1034	0.0618	4.8535	1.8569±0.001	[25, 27]
B0540-69	0.0505	1.6706	2.140±0.009	[28, 29]
J0537-6910	0.016	4.9328	-1.5	[30]
B1509-58	0.151	1.5648	2.839±0.001	[29, 31]
J1846-0258	0.3266	0.728	2.16 ±0.13	[32]
J1119-6127	0.408	1.6078	2.684±0.002	[33]
J1734-3333	1.1693	8.128	0.9±0.2	[34]

[18–20]. Notice that the moment of inertia is assumed to be constant, so that we can take it out from the parenthesis. Equation **2.5** tells us the dynamics of a neutron star in a vacuum medium with a dipole moment μ and inclination angle α. Apart from the spin-down torque there is another component of the MDR torque which forces alignment of the inclination angle

$$\frac{d}{dt}(I\alpha) = -\frac{2\mu^2\Omega^2}{3c^3}\sin\alpha\cos\alpha, \tag{2.6}$$

[21, 22]. The components of the torque given in Equation **2.5** and Equation **2.6** presume that outside the star the medium is vacuum. This is a gross simplification for a pulsar magnetosphere as it was soon shown by Goldreich & Julian (1969) that there exists a co-rotating plasma around a pulsar [23].

2.2 Braking Index

The braking index of a pulsar is defined as:

$$n \equiv \frac{\Omega\ddot{\Omega}}{\dot{\Omega}^2} \tag{2.7}$$

which is a dimensionless parameter describing the angular acceleration of a spinning-down pulsar. In Table 2.1, there are observed values of period, characteristic age and n values with references.

As it could be noticed, most of n are close to but less than 3. This implies that for the spin-down of a neutron star, Ω^3 dependence of the MDR model is basically correct, but that there would be other factors modifying the spin-down behaviour.

The second braking index, m is defined as

$$m \equiv \frac{\Omega^2 \ddot{\Omega}}{\dot{\Omega}^3} \quad \textbf{(2.8)}$$

and for a spin-down law of the form $\dot{\Omega} = K\Omega^n$ we have $m = n(n-1) + n^2$. For example, for the Crab pulsar $n = 2.51$ (see Table 2.1) gives $m_{n=2.51} = 2.51 \times 1.51 + 2.51^2 = 10.1$ which is very close to the observed value $m_{\text{obs}} = 10.2 \pm 0.1$ [24].

2.3 Characteristic Age

Equation **2.5** is of the form

$$\dot{\Omega} = -K\Omega^3 \quad \textbf{(2.9)}$$

where

$$K \equiv -\frac{2\mu^2 \sin^2\alpha}{3c^3 I}. \quad \textbf{(2.10)}$$

is a constant. If we integrate Equation **2.9** and eliminate K between the integrated form and Equation **2.9** we would derive

$$t = -\frac{\Omega}{2\dot{\Omega}}\left(1 - \frac{\Omega^2}{{\Omega_0}^2}\right). \quad \textbf{(2.11)}$$

If, Ω is much smaller then Ω_0, the term in parenthesis on the right hand side equals to unity. Then Equation **2.11** becomes:

$$\tau_{\text{c}} \equiv -\Omega/2\dot{\Omega} \quad \textbf{(2.12)}$$

which is a reasonable approximation for the age of a pulsar and called the characteristic age. Referring to the ATNF database [35]

$$\begin{aligned} \Omega &= 3.34 \times 10^{-2}\,(\text{s}^{-1}) \\ \dot{\Omega} &= -4.21 \times 10^{-13}\,(\text{dimensionless}) \end{aligned}$$

and so the characteristic age of the Crab Pulsar is:

$$\tau_c = -\frac{\Omega}{2\dot{\Omega}} = 1257\,(\text{years})$$

which is reasonably close to the real age of the Crab pulsar, 961 years.

The braking index is 3 only if the assumptions that μ, I and α remain constant; if α is changing w.r.t. time the braking index becomes

$$n = 3 - 4\dot{\alpha}\tau_{\text{c}}\cot\alpha. \quad \textbf{(2.13)}$$

If one calculates the braking index with the time derivative of α observed by Lyne et al. (2013) [8] as $\alpha = 45^\circ - 70^\circ$ for the vacuum medium, one obtains:

$$n_{45} = 2.46$$

$$n_{70} = 2.80.$$

If we plug Equation **2.6** into Equation **2.13**, then we get:

$$n = 3 + 2\cot^2\alpha, \tag{2.14}$$

[21, 22]. It's still assumed that the magnetic moment and the moment of inertia of the pulsar are constant.

2.4 Plasma model of the pulsars

Soon after it was established that pulsars are spinning down under MDR torques it was understood that the presumption of the vacuum medium is inadequate and that pulsars are surrounded by a co-rotating plasma [23] because of the driving electric and inducing magnetic fields. These fields can rip off electrons from the surface of the neutron star.

Oblique 3-D solution in plasma medium was first simulated by Spitkovsky (2006) [12]. By fitting the results of his numerical simulation in the force-free limit, he found the spin-down torque on the star as

$$\frac{d}{dt}(I\Omega) = -\frac{\mu^2\Omega^3}{c^3}(1+\sin^2\alpha). \tag{2.15}$$

Accordingly the braking index is

$$n = 3 - 4\dot{\alpha}\tau_c u \tag{2.16}$$

where

$$u(\alpha) \equiv \frac{\sin\alpha\cos\alpha}{1+\sin^2\alpha}, \tag{2.17}$$

and we assumed I is constant. If we use the value of time derivative of α obtained by Lyne et al. (2013) [8] as 0.0062° per year and calculate n for the plasma medium, we get:

$$n_{45} = 2.82$$

$$n_{70} = 2.91.$$

Recently, Philippov et al. [13] has shown that the torque acting on the pulsar in the plasma has a component forcing alignment as

$$\frac{d}{dt}(I\alpha) = -\frac{\mu^2\Omega^2}{c^3}\sin\alpha\cos\alpha. \tag{2.18}$$

Dividing Equation **2.15** by Equation **2.18** we get

$$\frac{d\ln\Omega}{d\alpha} = \frac{1+\sin^2\alpha}{\sin\alpha\cos\alpha}, \tag{2.19}$$

which can be solved by integrating both sides

$$\frac{\Omega}{\Omega_0} = \frac{\sin\alpha/\sin\alpha_0}{\cos^2\alpha/\cos^2\alpha_0}. \tag{2.20}$$

By plugging Equation **2.18** into Equation **2.16** we get

$$n = 3 + 2u^2(\alpha). \tag{2.21}$$

This form is similar with the Equation **2.14** indeed. As the object tends to align $n \geqslant 3$ for case of plasma medium just like the case of vacuum medium. Both MDR model in vacuum (with Equation **2.13**) and in plasma (Equation **2.16**), and also the recent simulations in plasma medium (with Equation **2.21**) by Philippov et al. [13] imply alignment and $n > 3$ although the observations suggest $n < 3$.

3. METHOD

As shown by Lyne et al. [8], the inclination angle of the Crab pulsar has been increasing at a rate of 0.62 degrees per century. MDR model and the plasma model both predict alignment, as the right hand side of Equation **2.18** is negative, in contradiction with this observation. A simple reason for the increasing inclination angle could be that the moment of inertia of the neutron star decreases, i.e. $\dot{I} \leqslant 0$. This would bring a positive term to the right hand side that may dominate the alignment term.

A possible cause for the decrease of the moment of inertia could be the reduction of the normal component of the crust while the superfluid component enlarges by the cooling of the object [36]. Indeed, we first considered this effect as the cause of the reduction of the moment of inertia. We have seen that this is a very small effect unable to explain the required rate of change in the moment of inertia for the observed rate of increase in the inclination angle. We have then considered the continuous reduction in the oblateness of the neutron star as a result of spin-down as a cause of the change in the moment of inertia. This also is not sufficient for explaining the observed rate of change of the inclination angle.

The Crab pulsar suffers star-quakes occurring on the crust of the NS. These quakes would create sudden increases in the rotation rate of the NS, followed by a recovery to its original rotation state [37, 38]. The crust is broken in during the star-quakes and becomes more spherical. As the shape changes, the moment of inertia changes as well.

This section discusses the spin evolution of the Crab pulsar in the presence of a change in the moment of inertia without referring to the cause of the change in the moment of inertia.

3.1 Spin down with decreasing moment of inertia

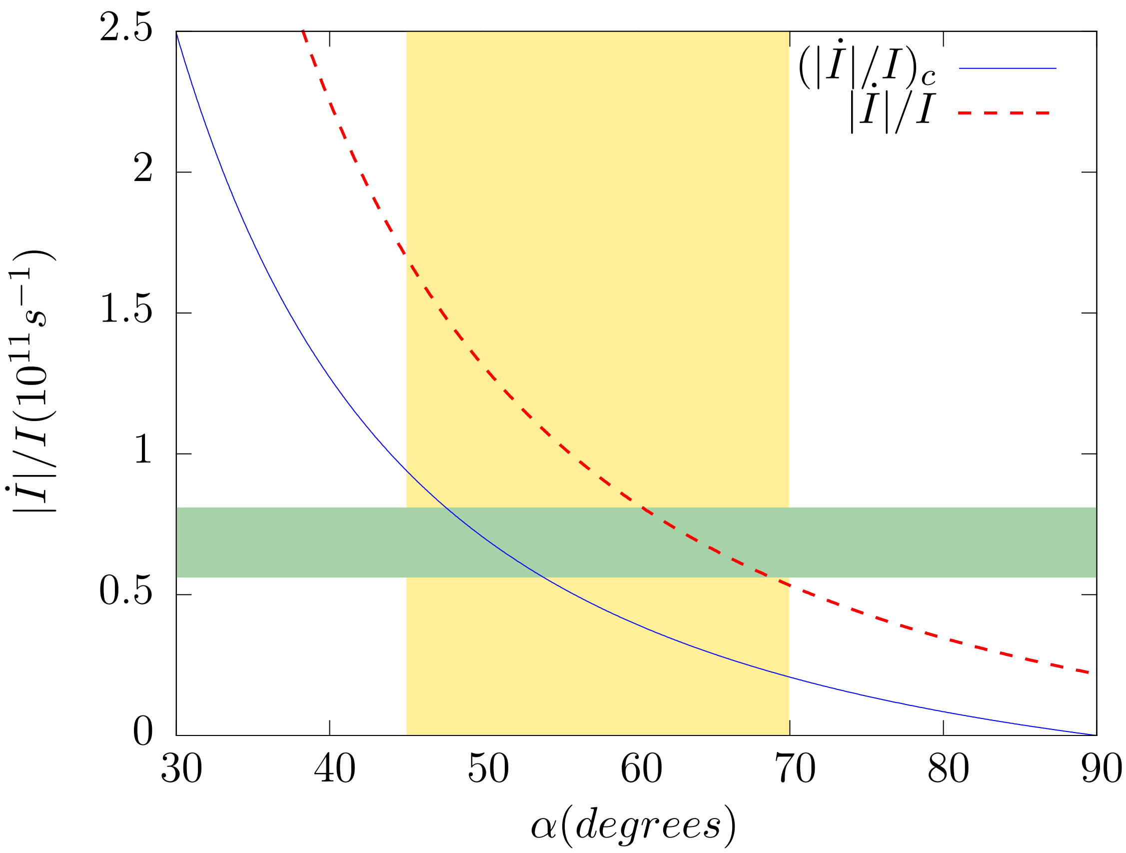

Figure 3.1: $|\dot{I}/I|$
Relative change in the moment of inertia required to explain the rate of increase in inclination angle as inferred by Equation **3.5** (dashed line) and the critical relative change in the moment of inertia given in Equation **3.4** (solid line). The vertical shaded region shows the range of inclination angle of the Crab pulsar measured [4–7] to be between 45-70 degrees. The horizontal shaded region shows $\langle|\dot{I}/I|\rangle = (0.686 \pm 0.124) \times 10^{-11}\ \mathrm{s}^{-1}$ inferred from the observed glitches via the star-quake model.

Assuming the moment of inertia of the neutron star changes in time, the equations describing the evolution of angular velocity and inclination angle, Equation **2.15** and Equation **2.18**, become

$$\dot{\Omega} = -\frac{\mu^2\Omega^3}{Ic^3}(1+\sin^2\alpha) - \frac{\dot{I}}{I}\Omega, \quad \textbf{(3.1)}$$

and

$$\dot{\alpha} = -\frac{\mu^2\Omega^2}{Ic^3}\sin\alpha\cos\alpha - \frac{\dot{I}}{I}\alpha, \quad \textbf{(3.2)}$$

respectively. If $\dot{I}/I < 0$ and dominates the first term on the right hand-side then $\dot{\alpha} > 0$. In this chapter we consider whether the counter alignment of the Crab pulsar at a rate of 0.62° per century could result from the decrease of its moment of inertia. Equation **3.2**

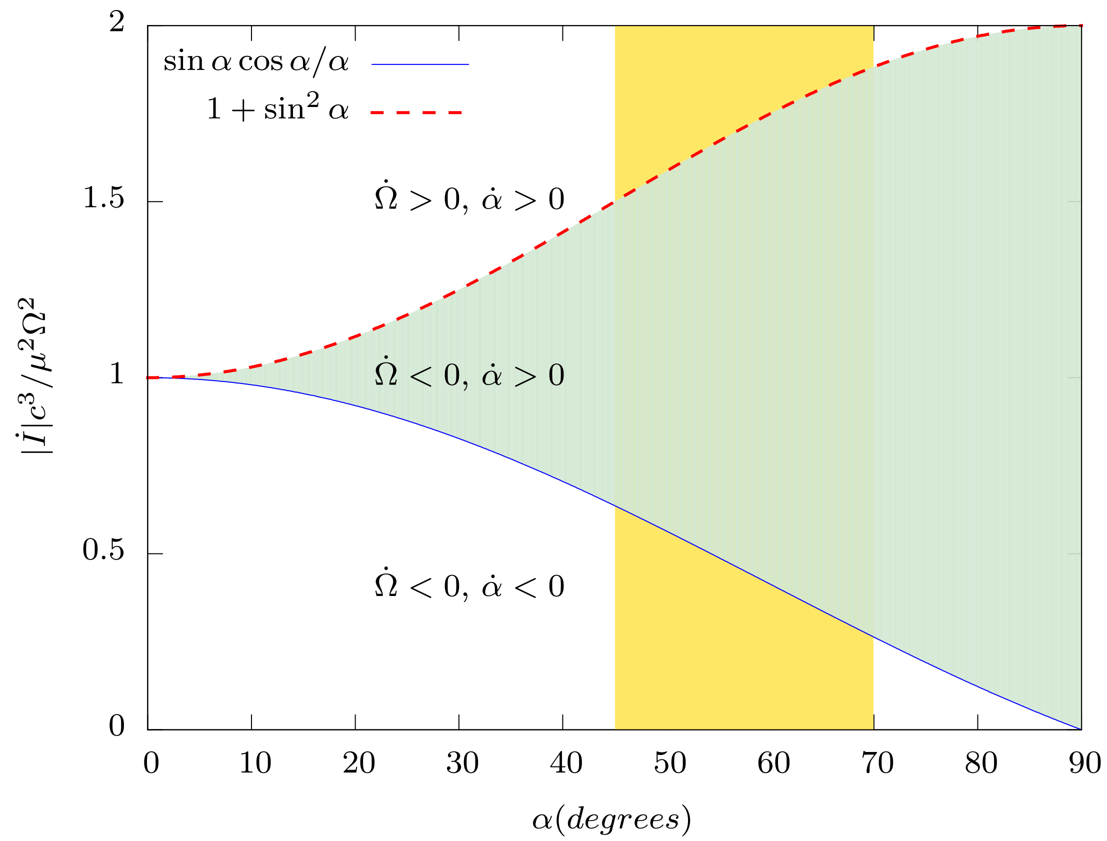

Figure 3.2: $|\dot{I}|c^3/m^2\Omega^2$
The dimensionless parameter combination $|\dot{I}|c^3/\mu^2\Omega^2 = 7.5 \times 10^{11}(|\dot{I}|/I)\mu_{30}^{-2}(\Omega/189.8\ \mathrm{s}^{-1})^{-2}$ versus the inclination angle. The vertical shaded region shows the range of inclination angle of the Crab pulsar measured [4–7] to be between $45-70$ degrees. The shaded region between the curves corresponds to the parameter range satisfying the condition given in Equation **3.7** i.e. that the condition for spin-down with increasing inclination angle. If the rate of change of moment of inertia is smaller (region below the solid line) corresponding to $\sin\alpha\cos\alpha/\alpha$ one may have $\dot{\alpha}<0$ while the star spins-down. The shaded region corresponding to the $\dot{\Omega}<0$ and $\dot{\alpha}>0$ phase is wider for large inclination angles implying that pulsars with large inclination angles will likely be in a state of counter-alignment. Pulsars with small inclination angles will more likely be in an alignment phase.

implies that the critical rate of change of moment of inertia for $\dot{\alpha}=0$ is

$$\left.\frac{|\dot{I}|}{I}\right|_{\mathrm{c}} = \frac{\mu^2\Omega^2}{Ic^3}\frac{\sin\alpha\cos\alpha}{\alpha}. \tag{3.3}$$

Eliminating $\mu^2\Omega^2/Ic^3$ between this equation and Equation **3.1** we obtain

$$\left.\frac{|\dot{I}|}{I}\right|_{\mathrm{c}} = -\frac{\dot{\Omega}}{\Omega}\frac{u(\alpha)}{\alpha-u(\alpha)} \tag{3.4}$$

where u is given in Equation **2.17**. Eliminating μ among Equation **3.1** and Equation **3.2** we obtain

$$\frac{\dot{I}}{I} = \frac{\dot{\alpha}-\frac{\dot{\Omega}}{\Omega}u(\alpha)}{\alpha+u(\alpha)}. \tag{3.5}$$

We define the timescale for the change of moment of inertia as

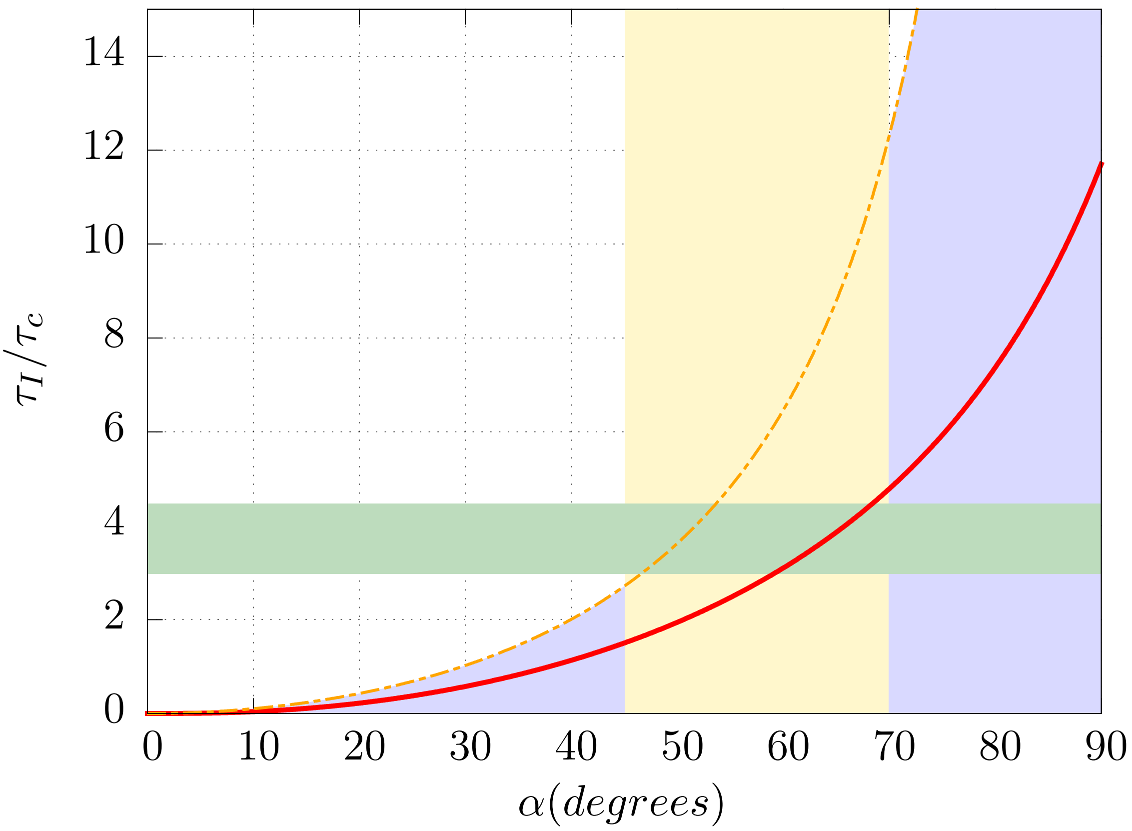

Figure 3.3: τ_I/τ_c
The ratio of the evolutionary time scale of the effective moment of inertia to the characteristic age of Crab, τ_I/τ_c, versus the inclination angle α. The vertical shaded region shows the range of inclination angle of the Crab pulsar measured [4–7] to be between 45-70 degrees. The shaded region under the the curve corresponds to the parameter range satisfying the condition given in Equation **3.8**. The horizontal shaded region is the range $\tau_I/\tau_c = 3.72 \pm 0.75$ where $\tau_I = (1.46 \pm 0.3) \times 10^{11}$ s is inferred from the glitch activity and $\tau_c = 1257$ yr is the characteristic age inferred from the spin-down. Solid line is the ratio corresponding to the measured value of $\dot{\alpha}$ as given in Equation **3.9**.

$$\tau_I \equiv \frac{I}{\dot{I}}. \tag{3.6}$$

For the different inclination angles measured 45° [6] and 70° [5], τ_I takes values as 0.5×10^{11} s and 2×10^{11} s, respectively. This is shown in Figure 3.1 (multiplicative inverse of y-axis). From Equation **3.1** with the constraint that $\dot{\Omega} < 0$ and from Equation **3.3** with the constraint $\dot{\alpha} > 0$ we find:

$$1 + \sin^2\alpha > \frac{|\dot{I}|c^3}{\mu^2\Omega^2} > \frac{(\sin\alpha\cos\alpha)}{\alpha} \tag{3.7}$$

This general inequality for plasma medium is shown in Figure 3.2 with the region between dashed and continuous lines.

By using Equation **3.1** again, the inequality becomes:

$$0 < \frac{\tau_I}{2\tau_c} < 2\alpha \frac{\sin\alpha\cos\alpha}{\alpha(1+\sin^2\alpha)} - 2 \quad \textbf{(3.8)}$$

We may also write the general rate of change of I with this τ_I/τ_c parameter as:

$$\frac{\tau_I}{\tau_c} = \frac{2(\alpha - u(\alpha))}{2\dot{\alpha}\tau_c + u(\alpha)}. \quad \textbf{(3.9)}$$

This last relation is shown in Figure 3.3 with the known values of τ_I and τ_c as $\tau_I = (1.46 \pm 0.3) \times 10^{11}$ s and $\tau_c = 1257$ years (as calculated above) respectively and $\tau_I/\tau_c = 3.68 \pm 0.75$.

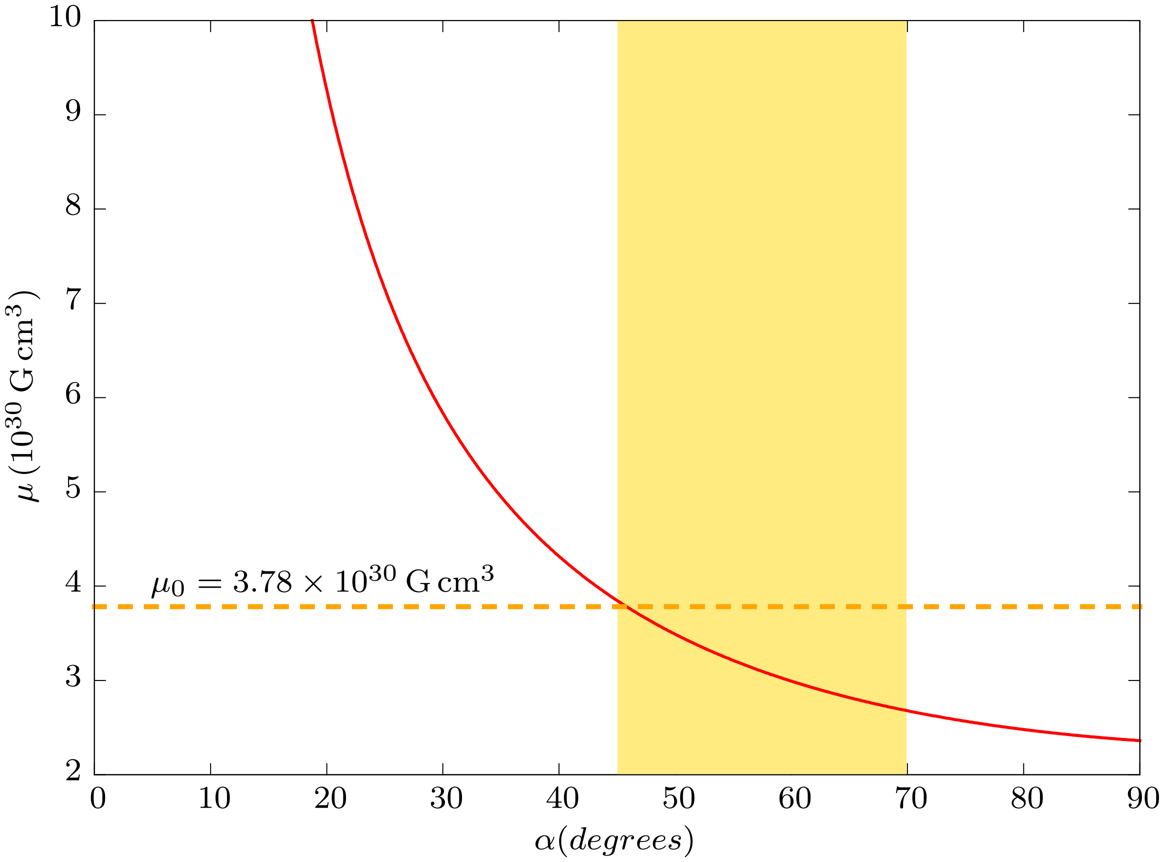

Figure 3.4: μ
The magnetic moment versus the inclination angle as inferred from Equation **3.10**. The vertical shaded region shows the range of inclination angle of the Crab pulsar measured [4–7] to be between 45-70 degrees. The horizontal line corresponds to the magnetic moment inferred from the orthogonal vacuum model, $\mu_0 = 3.78 \times 10^{30}$ G cm^3.

By plugging Equation **3.5** into Equation **3.1** one obtains:

$$\mu = \mu_0 \sqrt{\frac{2(\alpha + 2\dot{\alpha}\tau_c)}{3(\alpha - u(\alpha))(1+\sin^2\alpha)}} \quad \textbf{(3.10)}$$

where $\mu_0 = \sqrt{3c^3 I P\dot{P}/8\pi^2} = 3.78 \times 10^{30}\,\mathrm{G\,cm^3}$ is the usual magnetic dipole moment inferred with the orthogonal vacuum model Equation **2.5** and the observed P and $\dot{P}$

values. The change of μ against α is shown in Figure 3.4. By assuming a constant

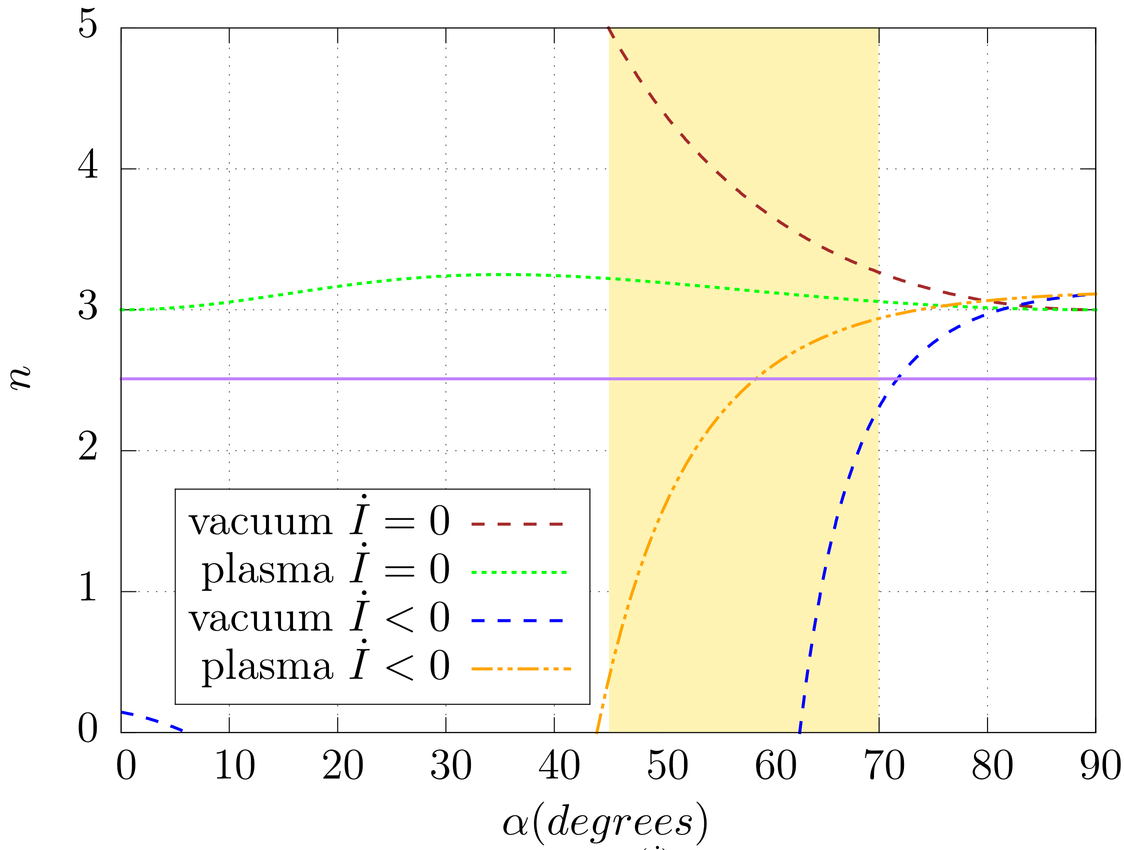

Figure 3.5: $n - \alpha\,(\dot{I})$
The braking index versus the inclination angle according to the vacuum model ($n = 3 + 2\cot^2\alpha$) (dashed line), the plasma filled model (dotted line) given in Equation **2.21** for constant moment of inertia, the vacuum model with changing moment of inertia (dashed line), and plasma filled model with changing moment of inertia (dot-dash line). For for the latter we have taken $n_I = 2$ a value such that the plasma filled model with changing moment of inertia can explain the braking index of the Crab pulsar $n = 2.51(1)$ which is shown by Lyne et al. (1993) [24] with the horizontal solid line.

rate of change of the moment of inertia $\tau_I = constant$ we can obtain a relation between the angular velocity and the inclination angle. Equation **3.1** and Equation **3.2** can be used to eliminate μ, as:

$$\frac{\dot{\Omega}}{\Omega} = \left(\dot{\alpha} - \frac{1}{\tau_I}\alpha\right)\left(\frac{1+\sin^2\alpha}{\sin\alpha\cos\alpha}\right) - \frac{1}{\tau_I} \tag{3.11}$$

where we used Equation **3.6**. As a result there exist some differences between the two forms of braking index in simple vacuum model and plasma filled model.

3.2 The effects of change of I to the braking index and second braking index

We obtain this counter alignment with a changing moment of inertia, above. In the plasma filled model with a changing moment of inertia, with the time derivative of

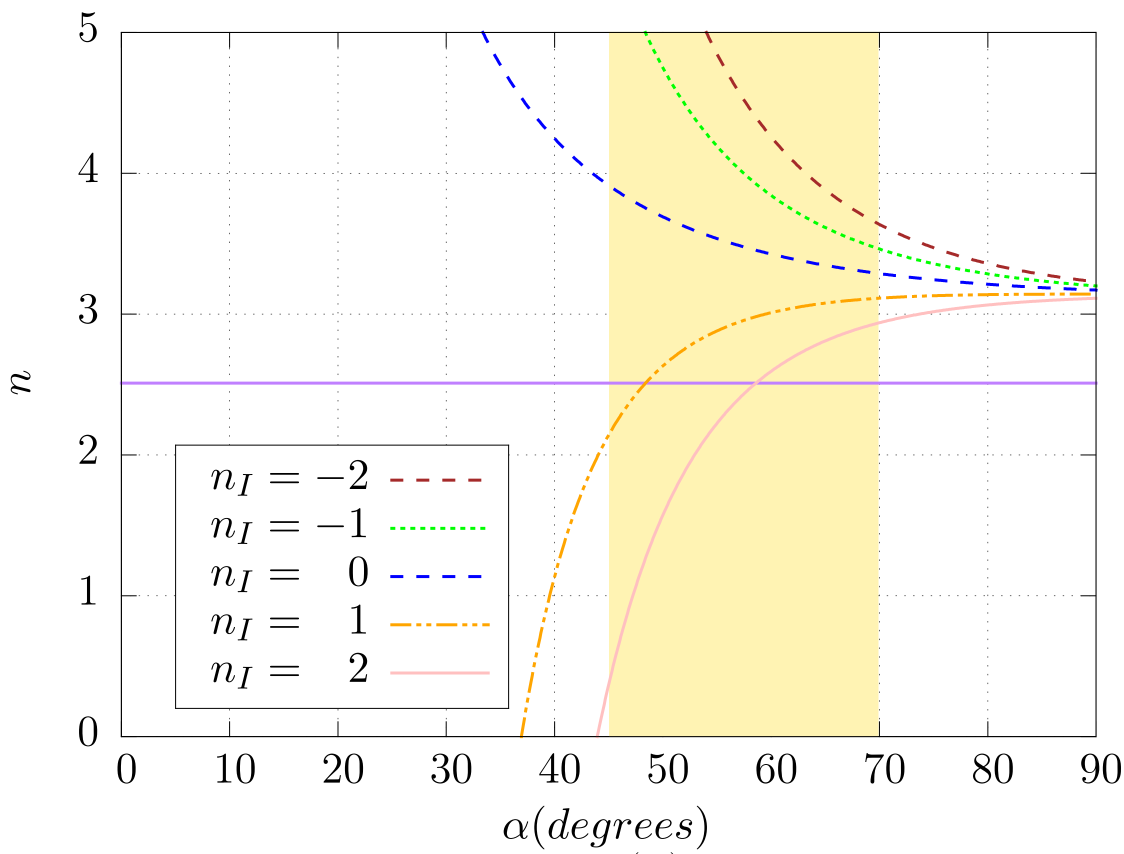

Figure 3.6: $n - \alpha\,(n_{\mathrm{I}})$
This figure explores the consequences of different values of n_I in the plasma-filled model with changing moment of inertia. The vertical shaded region shows the range of inclination angle of the Crab pulsar measured [4–7] to be between 45-70 degrees. The horizontal solid line shows the braking index of the Crab pulsar which is shown by Lyne et al. (1993) [24] as $n = 2.51(1)$.

Equation **3.1**, we obtain:

$$n = 3 + 2u^2 + \left(1 + 4u^2 - 2u\alpha\right)x + (2u^2 - 2u\alpha - n_I)x^2 \tag{3.12}$$

where

$$x \equiv \frac{\dot{I}\Omega}{I\dot{\Omega}} = 2\frac{\tau_c}{\tau_I}$$

and

$$n_I \equiv \frac{I\ddot{I}}{\dot{I}^2}$$

are both dimensionless parameters. This equation is visualized below in Figure 3.5 and Figure 3.6 for different models. Note that $x = 0$ corresponds to constant moment of inertia. In this case the last equation Equation **3.12** reduces to Equation **2.21**. From Equation **3.9** and the definition of x, it would also be written as:

$$x = \frac{2\dot{\alpha}\tau_c + u(\alpha)}{2(\alpha - u(\alpha))} \tag{3.13}$$

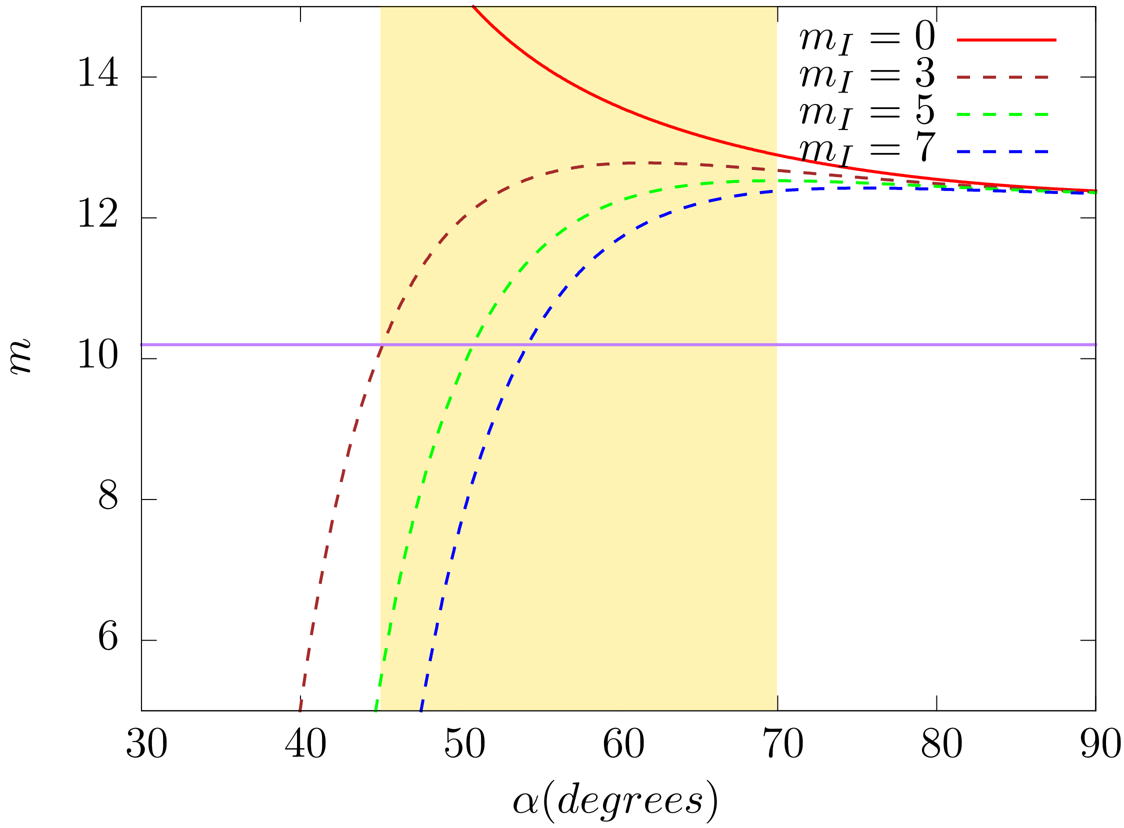

Figure 3.7: $m - \alpha(m_I)$
The second braking index versus the inclination angle according to Equation **3.14** for $n = 2.51$, $n_I = 1.5$ and for $m_I = 0$ (solid line), $m_I = 3$ (dashed line), $m_I = 5$ (dashed line) and $m_I = 7$ (dashed line). The measured second braking index of the Crab pulsar $m = 10.2(1)$ is shown by Lyne et al.(1993) [24] as the horizontal line.

Remember that for the MDR model, $n = 3$ and $m = 15$, while the observed result is $m = 10.2 \pm 0.1$ [24]. Again by Equation **3.1** and Equation **2.8**, one can derive this formula of m in terms of n_I, u, v, m_I, n and α:

$$\begin{aligned} m = & \left(-6u^2 + n_I + 4u^2 n_I + 4u^2 v + 2v\alpha^2 + 6u\alpha - m_I - 6v\alpha u - 4u\alpha n_I\right) x^3 \\ & + \left(-2u\alpha n_I - 1 + 2u\alpha - 12v\alpha u + 12u^2 v + 2v\alpha^2 + 4u^2 n_I - 6u^2\right) x^2 \\ & + \left(4u^2 n - 6v\alpha u + n - 2u^2 + 12u^2 v - 2u\alpha n\right) x \\ & - 3 + 4u^2 n + 6n - 2u^2 + 4u^2 v \end{aligned} \tag{3.14}$$

where

$$v(\alpha) = \frac{1 - 3\sin^2\alpha}{(1 + \sin^2\alpha)^2} \tag{3.15}$$

and

$$m_I = \frac{I^2 \dddot{I}}{\dot{I}^3}. \tag{3.16}$$

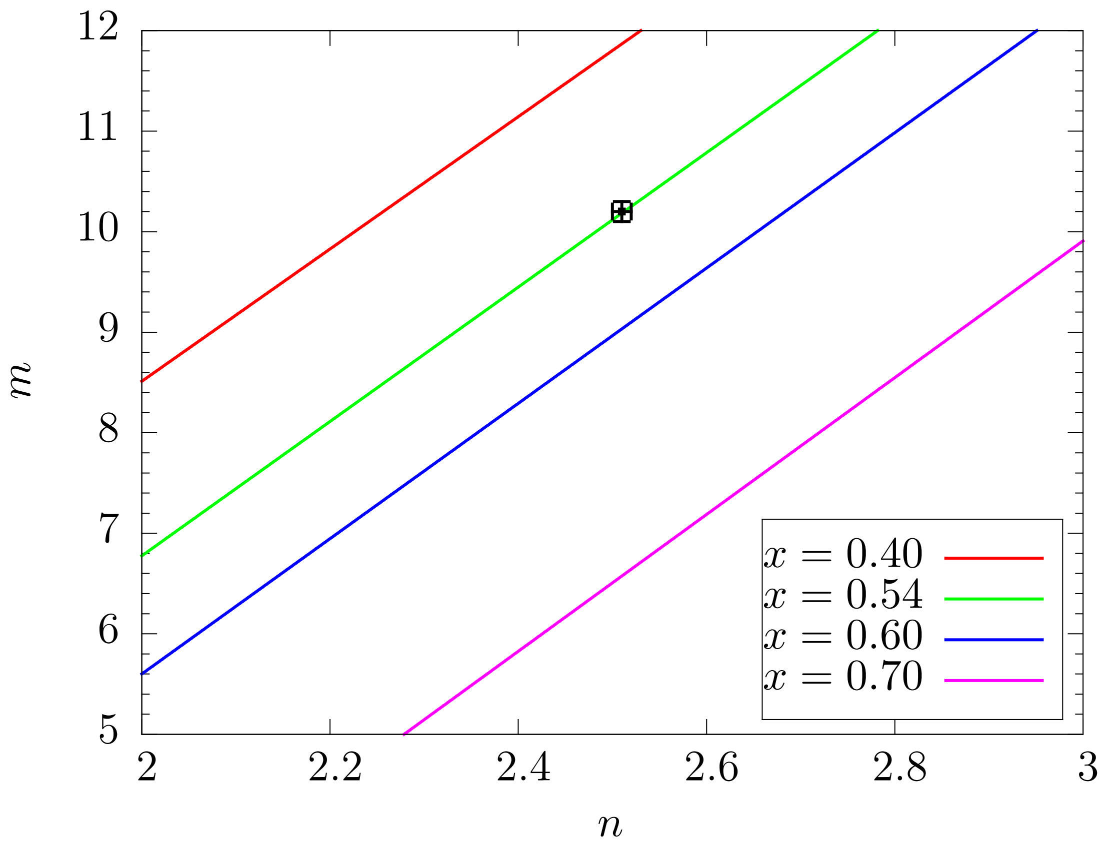

Figure 3.8: $m-n$
The second braking index versus the first braking index. For the point that takes the values of the Crab pulsar, $m = 10.2 \pm 0.1$ and $n = 2.51 \pm 0.01$, comparing m lines. x is a dimensionless parameter which is defined as $x = 2\tau_c/\tau_I$. Here, $x = 0.54$ is the line that m is on, where $m_I = 21.0$. This value would be changed by additional terms that can be plugged into Equation **3.1**, however, these are not within the scope of this thesis.

m_I is similar to m as n_I is similar to n. In Figure 3.7, the change of m w.r.t. α is shown for different m_I values. Figure 3.8 visualizes how m changes w.r.t. n.

4. CONCLUSION

In this thesis we studied the spin and inclination angle evolution of pulsars with changing moment of inertia, first for pulsars rotating in vacuum [16, 18] then for pulsars with a co-rotating plasma [12, 23]. The moment of inertia of pulsars might decrease as a result of glitch events. We have considered the possibility that the decreasing moment of inertia may be the underlying reason for the observed increasing inclination angle of the Crab pulsar [8]. We have seen that explaining the observed rate of increase, 0.62 degrees per century requires a decrease of moment of inertia at the rate $\dot{I} = -2.81 \times 10^{33}\,\mathrm{gcm}^2/\mathrm{s}$. We have considered whether the changing moment of inertia can also explain the braking index of the object measured to be $n = 2.51(1)$. We have found that the rate of changing of the $\dot{\Omega}$ is not sufficient to induce glitches. Then we decided to put pulsar wind and gravitational radiation terms into Equation **3.1** to obtain enough change in $\dot{\Omega}$ for a glitch

$$\begin{aligned}\dot{\Omega} = &-\frac{\mu^2\Omega^3}{Ic^3}(1+\sin^2\alpha) - 2.8\times 10^{13}\frac{\mu^2\Omega\kappa}{Ic}\left(\Omega\mu^8 R^{-5}/2\right)^{-1/7}\cos^2\alpha \\ &-\frac{4\times 10^{-4}\Omega}{t_{quake}} - \frac{(-4\times 10^{-6})^2 G I^{32/5}\Omega^5}{c^5},\end{aligned} \tag{4.1}$$

and Equation **3.2** becomes

$$\begin{aligned}\dot{\alpha} = &-\frac{\mu^2\Omega^2}{Ic^3}\left[1 - 2.8\times 10^{13}\frac{\mu^2\Omega\kappa}{Ic}\left(\Omega\mu^8 R^{-5}/2\right)^{-1/7}\right]\sin\alpha\cos\alpha \\ &-\frac{4\times 10^{-4}\Omega}{t_{quake}},\end{aligned} \tag{4.2}$$

where t_{quake} is the interval between two star-quakes and κ is a wind parameter, as well [39]. We also make a numerical simulation that evolves the Crab pulsar from the SN explosion to millions of years. This work is still ongoing. We have seen the Crab pulsar will evolve, on the $P - \dot{P}$ diagram towards the RRAT region.

REFERENCES

[1] **Baade, W. and Zwicky, F.** (1934). Cosmic Rays from Super-novae, *Proceedings of the National Academy of Science*, ***20***, 259–263.

[2] **Hewish, A.**, **Bell, S.J.**, **Pilkington, J.D.H.**, **Scott, P.F. and Collins, R.A.** (1968). Observation of a Rapidly Pulsating Radio Source, *Nature*, ***217***, 709–713.

[3] **Gold, T.** (1968). Rotating Neutron Stars as the Origin of the Pulsating Radio Sources, *Nature*, ***218***, 731–732.

[4] **Du, Y.J.**, **Qiao, G.J. and Wang, W.** (2012). Radio-to-TeV Phase-resolved Emission from the Crab Pulsar: The Annular Gap Model, *ApJ*, ***748***, 84, 1202.1096.

[5] **Dyks, J. and Rudak, B.** (2003). Two-Pole Caustic Model for High-Energy Light Curves of Pulsars, *ApJ*, ***598***, 1201–1206, astro-ph/0303006.

[6] **Harding, A.K.**, **Stern, J.V.**, **Dyks, J. and Frackowiak, M.** (2008). High-Altitude Emission from Pulsar Slot Gaps: The Crab Pulsar, *ApJ*, ***680***, 1378–1393, 0803.0699.

[7] **Watters, K.P.**, **Romani, R.W.**, **Weltevrede, P. and Johnston, S.** (2009). An Atlas for Interpreting γ-Ray Pulsar Light Curves, *ApJ*, ***695***, 1289–1301, 0812.3931.

[8] **Lyne, A.**, **Graham-Smith, F.**, **Weltevrede, P.**, **Jordan, C.**, **Stappers, B.**, **Bassa, C. and Kramer, M.** (2013). Evolution of the Magnetic Field Structure of the Crab Pulsar, *Science*, ***342***, 598–601, 1311.0408.

[9] **Beskin, V.S. and Nokhrina, E.E.** (2007). On the role of the current loss in radio pulsar evolution, *ApSS*, ***308***, 569–573, astro-ph/0608689.

[10] **Ruderman, M.A.** (1976). Crust-breaking by neutron superfluids and the VELA pulsar glitches, *ApJ*, ***203***, 213–222.

[11] **Contopoulos, I.**, **Kazanas, D. and Fendt, C.** (1999). The Axisymmetric Pulsar Magnetosphere, *ApJ*, ***511***, 351–358, astro-ph/9903049.

[12] **Spitkovsky, A.** (2006). Time-dependent Force-free Pulsar Magnetospheres: Axisymmetric and Oblique Rotators, *ApJ*, ***648***, L51–L54, astro-ph/0603147.

[13] **Philippov, A.**, **Tchekhovskoy, A. and Li, J.G.** (2014). Time evolution of pulsar obliquity angle from 3D simulations of magnetospheres, *MNRAS*, ***441***, 1879–1887, 1311.1513.

[14] **Wheeler, J.A.** (1966). Superdense Stars, *ARA&A*, ***4***, 393.

[15] **Pacini, F.** (1967). Energy Emission from a Neutron Star, *Nature*, ***216***, 567–568.

[16] **Deutsch, A.J.** (1955). The electromagnetic field of an idealized star in rigid rotation in vacuo, *Annales d'Astrophysique*, ***18***, 1.

[17] **Jackson, J.D.** (1962). *Classical Electrodynamics*, New York: Wiley.

[18] **Gunn, J.E. and Ostriker, J.P.** (1969). Magnetic Dipole Radiation from Pulsars, *Nature*, ***221***, 454–456.

[19] **Ostriker, J.P. and Gunn, J.E.** (1969). On the Nature of Pulsars. I. Theory, *ApJ*, ***157***, 1395.

[20] **Pacini, F.** (1968). Rotating Neutron Stars, Pulsars and Supernova Remnants, *Nature*, ***219***, 145–146.

[21] **Michel, F.C. and Goldwire, Jr., H.C.** (1970). Alignment of Oblique Rotators, *Astrophysical Letters*, ***5***, 21.

[22] **Davis, L. and Goldstein, M.** (1970). Magnetic-Dipole Alignment in Pulsars, *ApJ*, ***159***, L81–L86.

[23] **Goldreich, P. and Julian, W.H.** (1969). Pulsar Electrodynamics, *ApJ*, ***157***, 869.

[24] **Lyne, A.G.**, **Pritchard, R.S. and Graham-Smith, F.** (1993). Twenty-Three Years of Crab Pulsar Rotational History, *MNRAS*, ***265***, 1003.

[25] **Ng, C.Y. and Romani, R.W.** (2007). Birth Kick Distributions and the Spin-Kick Correlation of Young Pulsars, *ApJ*, ***660***, 1357–1374, astro-ph/0702180.

[26] **Dodson, R.G.**, **McCulloch, P.M. and Lewis, D.R.** (2002). High Time Resolution Observations of the January 2000 Glitch in the Vela Pulsar, *ApJ*, ***564***, L85–L88, astro-ph/0201005.

[27] **Roy, J.**, **Gupta, Y. and Lewandowski, W.** (2012). Observations of four glitches in the young pulsar J1833-1034 and study of its glitch activity, *MNRAS*, ***424***, 2213–2221, 1205.6264.

[28] **Livingstone, M.A.**, **Kaspi, V.M. and Gavriil, F.P.** (2005). Long-Term Phase-coherent X-Ray Timing of PSR B0540-69, *ApJ*, ***633***, 1095–1100, astro-ph/0507576.

[29] **Livingstone, M.A.**, **Kaspi, V.M.**, **Gavriil, F.P.**, **Manchester, R.N.**, **Gotthelf, E.V.G. and Kuiper, L.** (2007). New phase-coherent measurements of pulsar braking indices, *ApSS*, ***308***, 317–323, astro-ph/0702196.

[30] **Middleditch, J.**, **Marshall, F.E.**, **Wang, Q.D.**, **Gotthelf, E.V. and Zhang, W.** (2006). Predicting the Starquakes in PSR J0537-6910, *ApJ*, ***652***, 1531–1546, astro-ph/0605007.

[31] **Livingstone, M.A. and Kaspi, V.M.** (2011). Long-term X-Ray Monitoring of the Young Pulsar PSR B1509-58, *ApJ*, ***742***, 31, 1110.1312.

[32] **Livingstone, M.A.**, **Ng, C.Y.**, **Kaspi, V.M.**, **Gavriil, F.P. and Gotthelf, E.V.** (2011). Post-outburst Observations of the Magnetically Active Pulsar J1846-0258. A New Braking Index, Increased Timing Noise, and Radiative Recovery, *ApJ*, ***730***, 66, 1007.2829.

[33] **Weltevrede, P.**, **Johnston, S. and Espinoza, C.M.** (2011). The glitch-induced identity changes of PSR J1119-6127, *MNRAS*, ***411***, 1917–1934, 1010.0857.

[34] **Espinoza, C.M.**, **Lyne, A.G.**, **Kramer, M.**, **Manchester, R.N. and Kaspi, V.M.** (2011). The Braking Index of PSR J1734-3333 and the Magnetar Population, *ApJ*, ***741***, L13, 1109.2740.

[35] **Manchester, R.N.**, **Hobbs, G.B.**, **Teoh, A. and Hobbs, M.** (2005). The Australia Telescope National Facility Pulsar Catalogue, *AJ*, ***129***, 1993–2006, http://www.atnf.csiro.au/people/pulsar/psrcat/, astro-ph/0412641.

[36] **Ho, W.C.G. and Andersson, N.** (2012). Rotational evolution of young pulsars due to superfluid decoupling, *Nature Physics*, ***8***, 787–789, 1208.3201.

[37] **Espinoza, C.M.**, **Lyne, A.G.**, **Stappers, B.W. and Kramer, M.** (2011). A study of 315 glitches in the rotation of 102 pulsars, *MNRAS*, ***414***, 1679–1704, 1102.1743.

[38] **Yu, M.**, **Manchester, R.N.**, **Hobbs, G.**, **Johnston, S.**, **Kaspi, V.M.**, **Keith, M.**, **Lyne, A.G.**, **Qiao, G.J.**, **Ravi, V.**, **Sarkissian, J.M.**, **Shannon, R. and Xu, R.X.** (2013). Detection of 107 glitches in 36 southern pulsars, *MNRAS*, ***429***, 688–724, 1211.2035.

[39] **Gugercinoglu, E.**, **Andac, C.**, **Eksi, K.Y. and Alpar, M.A.**, (2015). Crab pulsar's inclination angle increasing by decreasing effective moment of inertia via starquakes, in preparation.

CURRICULUM VITAE

Name Surname: İbrahim Ceyhun Andaç

Place and Date of Birth: İzmir, Turkey, 22.02.1988

Adress: Physics Engineering Department, Faculty of Science and Letters, Istanbul Technical University, TR-34469, Maslak–Istanbul, Turkey

E-Mail: andac@itu.edu.tr

B.Sc.: Istanbul Technical University, Physics Engineering Department